VANDERMONDE INVARIANCE TRANSFORMATION

Tobias P. Kurpjuhn *kurpjuhn@nws.ei.tum.de*
Michel T. Ivrlač *ivrlac@nws.ei.tum.de*
Josef A. Nossek *nossek@nws.ei.tum.de*

Institute for Circuit Theory and Signal Processing
Technische Universität München, Munich, Germany

ABSTRACT

In this article we introduce a novel multiple-input-multiple-output (MIMO) spatial filter (SF) which can be applied as a preprocessing scheme to uniform linear arrays, preserving the Vandermonde structure of the steering vectors while changing the amplitude and the phase gradient of the steering vector in a nonlinear fashion. The new scheme is therefore titled Vandermonde Invariance Transformation.

The introduced degrees of freedom due to this preprocessing transformation can be used to beneficially influence the properties of the channel to achieve an enhanced performance of the subsequent signal processing algorithm.

1. INTRODUCTORY MOTIVATION

Some years ago the application of antenna arrays has been proposed for mobile communication systems to attain an increase in capacity and interference reduction by additionally exploiting the spatial separation of the mobile users.
Using more then one antenna for the receiver and/or sender provokes a noticeable increase of the system performance by achieving antenna gain, enhanced interference cancellation, and also transmit-receive diversity. Exploiting these properties requires the knowledge of the channel. Therefore channel estimation has to be applied to determine the parameters of the channel. These channel estimation schemes work better for higher signal-to-noise ratios (SNR). To this end preprocessing schemes can be applied to the antenna output to amplify the user signal over the noise and interference.

The most commonly used structure of an antenna array is the *Uniform Linear Array* (ULA). In this case M antennas are arranged in a line with equal distance to their neighboring antennas. Assuming L different propagation paths impinging at a ULA with M antennas under the influence of additive, possibly colored noise produces the data model

$$\mathbf{x}(t) = \sum_{n=1}^{L} \rho_n \cdot \mathbf{a}_n \cdot s_n(t) + \mathbf{n}(t), \tag{1}$$

where ρ_n, $\mathbf{a}_n$, $s_n(t)$, and $\mathbf{n}(t)$ denote the complex amplitude of path n, the steering vector of path n, the arriving signal of path n, and complex, possibly colored noise, respectively.
Under the assumption of discrete wavefronts [1], the steering vectors $\mathbf{a}_n$ are parameterized only by one angle ϕ_n between the propagation path and the ULA. The steering vector can be written as

$$\mathbf{a}_n = \left[1, \mathrm{e}^{\mathrm{j}\mu_n}, \cdots, \mathrm{e}^{\mathrm{j}(M-1)\mu_n}\right]^{\mathrm{T}}, \tag{2}$$

where $()^{\mathrm{T}}$ denotes transposition and $\mu_n = -2\pi\Delta\sin\phi_n$ is the spatial frequency with the antenna spacing Δ in fractions of the wavelength. Rewriting eq. (1) in vector-matrix notation leads to

$$\mathbf{x}(t) = \mathbf{A} \cdot \mathrm{diag}\{\rho_n\}_{n=1}^{L} \cdot \mathbf{s}(t) + \mathbf{n}(t). \tag{3}$$

In the following we will derive a transformation matrix $\mathbf{T} \in \mathbb{C}^{M\times M}$ which is applied to the data vector $\mathbf{x}(t)$. The new output reads as

$$\mathbf{y}(t) = \underbrace{\mathbf{T}\cdot\mathbf{A}}_{\mathbf{B}} \cdot \mathrm{diag}\{\rho_n\}_{n=1}^{L} \cdot \mathbf{s}(t) + \underbrace{\mathbf{T}\cdot\mathbf{n}(t)}_{\tilde{\mathbf{n}}(t)}. \tag{4}$$

Thereby, we design $\mathbf{T}$ such, that the matrix $\mathbf{B}$ is again a steering matrix of a ULA having Vandermonde structure. The vector $\mathbf{y}$ can be regarded as the output of a virtual ULA with noise $\tilde{\mathbf{n}}(t)$.

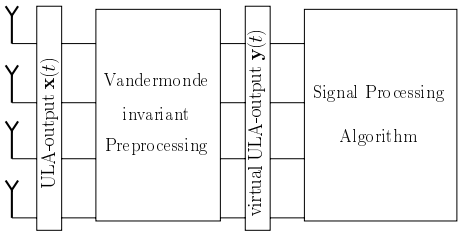

Fig. 1. Scheme of the proposed preprocessing transformation at the receiving antenna array.

2. VANDERMONDE INVARIANCE TRANSFORMATION

We start with two Vandermonde vectors $\mathbf{x}, \mathbf{y} \in \mathbb{C}^M$

$$\mathbf{x} = [1, x, x^2, \ldots, x^{M-1}]^{\mathrm{T}}$$

$$\mathbf{y} = c(x) \cdot [1, y, y^2, \ldots, y^{M-1}]^{\mathrm{T}}$$

where x and y are unimodular complex numbers

$$x = \mathrm{e}^{\mathrm{j}\mu}; \quad y = \mathrm{e}^{\mathrm{j}\nu}; \quad \mu, \nu \in \mathbb{R} \tag{5}$$

and $c(x)$ is the amplitude function, that is usually nonlinear with respect to x. In the sequel we will investigate matrices $\mathbf{T} \in \mathbb{C}^{M\times M}$ that map $\mathbf{x}$ to $\mathbf{y}$:

$$\mathbf{y} = \mathbf{T} \cdot \mathbf{x} \tag{6}$$

Matrices having this property will be called *Vandermonde Invariant Matrices*, the transformation from $\mathbf{x}$ to $\mathbf{y}$ *Vandermonde Invariance Transformation* (VIT). After the vector-matrix multiplication the n-th component y_n of vector $\mathbf{y}$ is a polynomial in x, that we will write in sum and product form

$$y_n = \sum_{p=1}^{M} t_{n,p} \cdot x^{p-1} \;=\; b_n \cdot \prod_{p=1}^{M-1} (x - r_{n,p}), \qquad (7)$$

where $r_{n,p} \in \mathbb{C}$ are the complex roots of the polynomials $y_n(x)$ and $b_n \in \mathbb{C}$ is a scaling factor. For $\mathbf{T}$ to be a Vandermonde invariant matrix, it must provide the vector $\mathbf{y}$ with the property

$$\mathrm{e}^{\mathrm{j}\nu} \;=\; \frac{y_{n+1}}{y_n} = \frac{b_{n+1}}{b_n} \cdot \frac{\prod_{p=1}^{M-1} (x - r_{n+1,p})}{\prod_{p=1}^{M-1} (x - r_{n,p})} =: H(x). \qquad (8)$$

This equation must hold for all complex values of x on the unit circle. We can split this condition into its absolute value and its angle. The absolute value of the right hand side has to be constant for all possible values of $|x| = 1$. To fulfill this equation we find a correspondence in filter theory. The only class of filter functions satisfying a constant absolute value for the whole frequency range are the all-pass functions. It is well known, that the poles and zeros of an all-pass function have to be symmetric with respect to the unit circle. The distribution of the poles and zeros can further be inspected by considering the angle of (8). The angle condition requires, that two subsequent rows of $\mathbf{y}$ are related by the same change of the angle. This requires, that two subsequent rows are related by the same transfer function H(x), hence

$$\frac{y_{\mathrm{M}}}{y_1} = H^{M-1}(x). \qquad (9)$$

As the total number of zeros in (7) is $(M-1)$, H(x) must be an all-pass function of first order

$$H(x) = \frac{b_{n+1}}{b_n} \cdot \frac{x - r^*}{x - r}, \qquad (10)$$

where $b_{n+2} \cdot b_n = b_{n+1}^2$ and $()^*$ denotes the mirror operator on the unit circle. This leads to

$$r_{n,p} = \begin{cases} r & \text{for } p \geq n \\ r^* & \text{else} \end{cases} \qquad (11)$$

For convenience we require, that (6) maps an all-ones vector again onto an all-ones vector, which translates to

$$b_n = (1-r)^{n-M} \cdot (1-r^*)^{1-n} \qquad (12)$$

Plugging (12), (11) and (5) into (7) gives the transformed vector $\mathbf{y}$ from (6) in its compact form as

$$\mathbf{y} \;=\; \mathbf{T} \cdot \mathbf{x} \;=\; \underbrace{\left(\frac{\mathrm{e}^{\mathrm{j}\mu} - r}{1 - r}\right)^{M-1}}_{c(\mu)} \cdot \begin{pmatrix} 1 \\ \mathrm{e}^{\mathrm{j}\nu} \\ \vdots \\ \mathrm{e}^{\mathrm{j}\nu(M-1)} \end{pmatrix}. \qquad (13)$$

Note that there is just one degree of freedom remaining.

3. SOME PROPERTIES OF THE VANDERMONDE INVARIANCE TRANSFORMATION

In this Section we will investigate two interesting properties of the VIT. For simplicity we restrict our consideration to real-valued roots r for constructing a Vandermonde invariant matrix $\mathbf{T}$.

3.1. Phase amplification

Recall that the variables x and y have been defined on the unit circle: $x = \mathrm{e}^{\mathrm{j}\mu}$ and $y = \mathrm{e}^{\mathrm{j}\nu}$ with $\mu, \nu \in [-\pi, \pi]$. From (10) and (12) follows, that ν can be expressed as a function of μ and r as follows

$$\nu \;=\; \arctan\left(\frac{\left(r - \frac{1}{r}\right) \cdot \sin\mu}{-2 + \left(r + \frac{1}{r}\right) \cdot \cos\mu}\right). \qquad (14)$$

See also Figure 2.

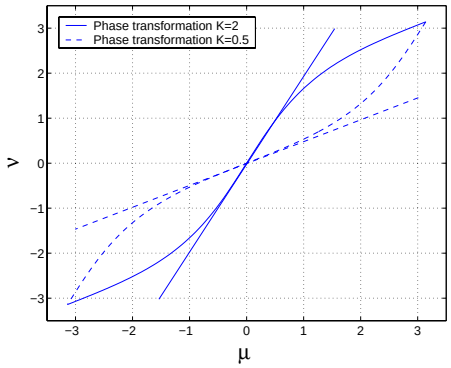

Fig. 2. Plot of the phase transformation for $K = 2$ and K=1/2.

Note that $\mu = 0$ is mapped to $\nu = 0$. At this point the second derivative of ν with respect to μ vanishes. This indicates, that the nonlinear relation (14) may be linearly approximated in the vicinity of $\mu = 0$ as

$$\nu_{\,\mathrm{lin}} = K \cdot \mu, \qquad (15)$$

with phase amplification $K = (r+1)/(r-1)$.

3.2. Amplitude amplification

While the norm of the input vector $\mathbf{x}$ is always constant to $||\mathbf{x}||_2 = \sqrt{M}$, the norm of the transformed vector $\mathbf{y}$ depends on μ in a nonlinear fashion. Using (13) we can write the squared norm of $\mathbf{y}$ as

$$||\mathbf{y}||_2^2 \;=\; M \cdot 2^{1-M} \cdot \left(1 + K^2 + (1 - K^2)\, \cos\mu\right)^{M-1}. \qquad (16)$$

From this it is clear that for $\mu = 0$ the norms of $\mathbf{y}$ and $\mathbf{x}$ are identical, whereas the amplitude for $\mu \neq 0$ heavily depends on K and μ. E.g.

$$||\mathbf{y}(\mu = \pi)||_2^2 \;=\; M \cdot K^{2M-2}. \qquad (17)$$

The ratio of the maximum and the minimum value of $||\mathbf{y}||_2^2$ is

$$\frac{\max\left\{||\mathbf{y}||_2^2\right\}}{\min\left\{||\mathbf{y}||_2^2\right\}} = \left(\max\left\{|K|, \frac{1}{|K|}\right\}\right)^{2M-2} \qquad (18)$$

and is therefore exponential in M but only polynomial in $|K|$ or $\frac{1}{|K|}$, respectively.

4. INTERPRETATION

4.1. Virtual Arrays and Nonlinear Channel Transformation

Assuming a single planar wave arriving at the ULA at an azimuth angle of ϕ and carrying a narrow-band baseband signal $s(t)$, the array output $\mathbf{x}(t)$ reads in the absence of noise as

$$\mathbf{x}(t) = \begin{bmatrix} 1 & e^{j\mu} & \dots & e^{j(M-1)\mu} \end{bmatrix}^T \cdot s(t). \qquad (19)$$

Since (19) is a Vandermonde vector its structure is not changed by premultiplication with a Vandermonde invariant matrix $\mathbf{T}$. Recalling (13) and (14) we see that the vector $\mathbf{y}$ is the output vector of a *virtual array*, that operates in a different environment (channel), since the spatial characteristics of the real and virtual array, represented by the spatial frequencies μ and ν, respectively, are different. Since (14) is nonlinear with respect to μ the spatial properties are changed in a nonlinear fashion, which leads to a *nonlinear channel transformation*. The change in the norms of the array output vectors $\mathbf{x}$ and $\mathbf{y}$ due to the VIT may be interpreted in two different ways.
Either the angular response (radiation pattern) of the virtual array has changed, or alternatively the channel has changed its angular amplitude characteristic just like the spatial frequency (phase) characteristic before.

4.2. Adaptive Antenna Aperture Zoom

When looking at the linear region of (14) around $\mu = 0$, the spatial separation $\Delta\mu$ of two wavefronts looks like $\Delta\nu = K \cdot \Delta\mu$ at the virtual array. If $|K| > 1$ we get a zooming effect, similar to the one of an optical lens:

$$\nu_{\text{lin}} = -2\pi \frac{K \cdot \Delta}{\lambda} \sin\phi. \qquad (20)$$

The expression $\frac{K \cdot \Delta}{\lambda}$ can be seen as an increase of the effective antenna spacing for a region in the vicinity of $\mu = 0$. For this particular region the antenna aperture is virtually increased. However, the increasing phase amplification leads also to a reduction of the size of the region of linearity. As in an optical system this effect corresponds to the decrease of depth of focus by increasing focal length.

Unfortunately this software zoom effect comes at rather a high price, since it leads to a large amplification of noise power. On the other hand using a phase attenuation (inverse-zoom), a considerable noise suppression may be achieved at a fairly low price, which will be shown in the next subsection and will form the basis of applications described in the next section.

4.3. Noise Shaping

Assume a ULA with omni-directional antennas that only receives spatially white noise of unity power density. The power density measured at the virtual array is given by the squared norm of its output vector, c.f. (16). This means, that for $|K| \neq 1$ the spatial distribution of noise power density will change due to the VIT, hence noise changes its color. This effect will be called *noise shaping* and is illustrated in Figure 3 which shows the spatial power

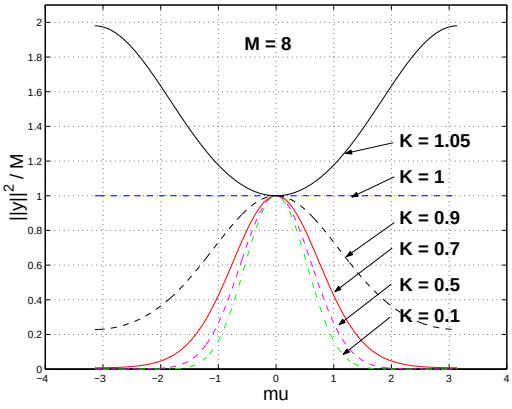

Fig. 3. Spatial noise power density at the output of the virtual 8-ULA for different values for the phase amplification K. Spatially white noise with unity power density is assumed at the input.

density of transformed white noise at the output of the virtual array for $M = 8$ antennas. First of all it shows, that even for a small positive zoom effect (here $K = 1.05$) the penalty in noise amplification is severe and gets even worse, by increasing the antenna number M. On the other hand even a very moderate loss of phase amplification, e.g. $K = 0.9$ leads to a considerable suppression of noise.
To better understand the noise suppression effect of noise shaping we have a look at the total noise power P at the output of the virtual array when the noise is of unity power density and white with respect to μ. Choosing $|K| < 1$ leads to an effective gain in SNR as can be seen from Table 1. However the noise covariance matrix is changed into $\tilde{\mathbf{R}}_N = \mathbf{T} \cdot \mathbf{R}_N \cdot \mathbf{T}^H$.

Searching for a optimum K we have to keep in mind, that we want to have a low P value to achieve as much noise suppression as possible and we simultaneously want to have $|K|$ close to 1, in order to get a low phase attenuation. In trying to fulfill both conditions simultaneously we maximize the cost function $\frac{K^2}{P}$. Note that P is a value of second order. The optimum value settles to $K_{opt} \approx 0.8$ largely independent of the ULA size M.

4.4. Multiple-Input Multiple-Output Spatial Filter

In contrast to the classical form of a spatial filter, which maps a vector input to a scalar output, the VIT maps vectors onto vectors, and therefore is a MIMO spatial filter. The VIT can also be thought of as a bank of spatial filters, that have tuned phase and amplitude relationships to preserve the Vandermonde structure of the input signal. Note that the VIT is linear in terms of its input and output Vandermonde vectors, but nonlinear in terms of their spatial frequencies.

$\|K\|$	1	0.9	0.8	0.7	0.5	0.1	$\to 0$
ΔSNR	0	2.5	4.2	5.1	6.10	6.76	6.79

Table 1. Noise suppression in dB due to noise shaping for different phase amplifications and $M = 8$

5. APPLICATION EXAMPLE

5.1. VAP-DOA Algorithm

In the conventional setup, N samples of the ULA output $\mathbf{x}(t) \in \mathbb{C}^M$ are measured at successive time instants and collected into a data matrix $\mathbf{X} \in \mathbb{C}^{M \times N}$ [2]. The measured data is then fed into one of the well known high resolution DOA estimation algorithms like MUSIC or ESPRIT [3, 2] that returns a set of estimated directions of arrival $\{\hat{\mu}_1, \ldots, \hat{\mu}_L\}$[1]. The quality of estimation depends on the reliability of the measured array output, i.e. the SNR, and also on the number of snapshots N that can be obtained during the coherence time of the channel. By introducing a VIT based preprocessing scheme we can achieve the same accuracy at a lower SNR level and/or with fewer snapshots. The second property enables us to track DOAs of faster changing channels.
This idea of *Virtual Array Processing* (VAP) is to start with raw estimates of L directions of arrival and then sequentially apply a set of VITs that are focused on these estimated directions, followed by subsequent DOA estimations based on the transformed data set. Due to the noise shaping effect of VIT this will lead to a more accurate estimate, for the price of a $L+1$ times higher computational load.

5.2. Simulation Results

We assume one wavefront impinging from $\phi = 27^o$ at an 8-ULA with $\Delta = 0.5$ spacing in spatially white noise and being estimated with the Standard ESPRIT algorithm. In the sequel we will compare the performance of the ESPRIT algorithm to its VAP variant. Figure 4 shows the RMSE of Standard ESPRIT as a function of the SNR. The upper line corresponds to the estimation without preprocessing and the lower line to the case of VAP enhanced estimation for $K = 0.8$. The simulation validated the previous results, that a choice of $K = 0.8$ is optimal in terms of lowest RMSE. For this value of K the VAP enhanced estimation achieves a gain in SNR of approximately 2 dB for a reasonable SNR range.
If we plot the RMSE as a function of the number of samples N,

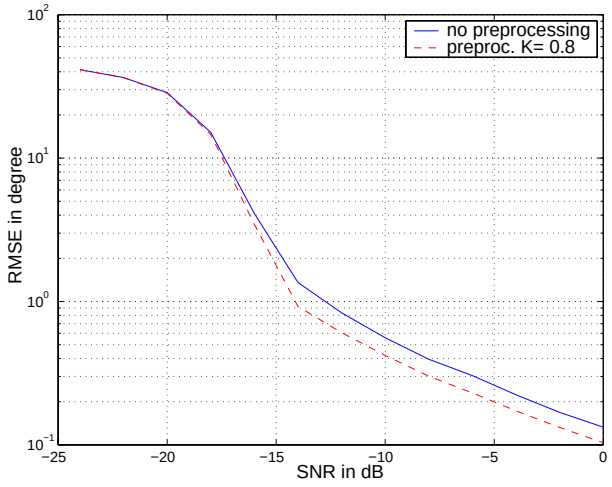

Fig. 4. RMSE of one wavefront from $\phi = 27^o$.

[1]The number of wavefronts L results from a model-order detection.

we get the plot shown in Figure 5. In the case of four wavefronts we can see that we gain a factor of approximately 1.33 with respect to the number of samples, which means a 25% reduction in the sample count and a 33% higher velocity threshold for moving objects.

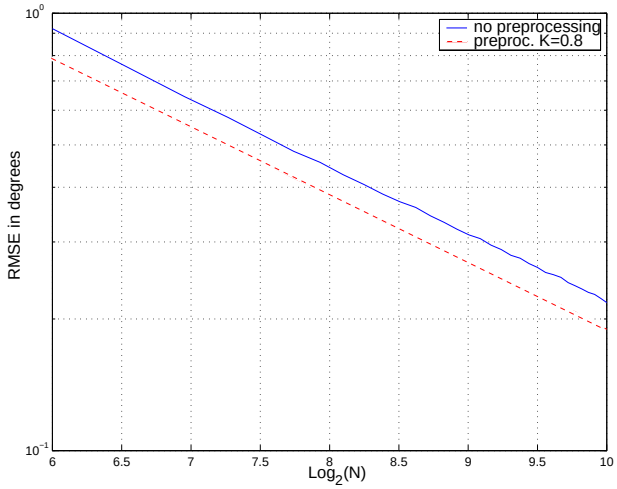

Fig. 5. RMSE of four wavefronts $\phi = \{-32^o, 2^o, 8^o, 57^o\}$ with a SNR of 5dB at an 8-ULA as a function of the samples N.

6. CONCLUSION

A novel class of MIMO spatial filters was introduced that well suites as a preprocessing scheme for signal processing algorithms operating on ULAs. These filters preserve the Vandermonde structure of the ULA steering vectors while changing their amplitude and phase-gradient in a nonlinear fashion. The filters can be described by means of the introduced VIT, which may be seen both as linear and non-linear. Effects like noise-shaping can be used to achieve enhanced performance of subsequent signal processing algorithms. Simulation results for a proposed enhancement of DOA estimation show that substantial gains in performance can be achieved.

7. REFERENCES

[1] J. J. Blanz and P. Jung, "A flexibly configurable spatial model for mobile radio systems," *IEEE Trans. Communications*, vol. 46, pp. 367–371, Mar. 1998.

[2] R. Roy and T. Kailath, "ESPRIT - estimation of signal parameters via rotational invariance techniques," *IEEE Trans. Acoustics, Speech, and Signal Processing*, pp. 984–995, July 1989.

[3] R.O. Schmidt, "Multiple emitter location and signal parameter estimation," *Proc. RA DC Spectrum Estimation Workshop*, vol. 34, pp. 276–280, March 1986.